NASA Technical Memorandum 81862

SUPPLEMENT TO: A COMPUTER PROGRAM FOR THE DESIGN AND ANALYSIS OF LOW-SPEED AIRFOILS

Richard Eppler and Dan M. Somers

DECEMBER 1980

National Aeronautics and Space Administration

Langley Research Center
Hampton, Virginia 23665

1 Report No.	2. Government Accession No.	3. Recipient's Catalog No.
NASA TM-81862		

4. Title and Subtitle	5. Report Date
Supplement To: A Computer Program for the Design and Analysis of Low-Speed Airfoils	December 1980
	6. Performing Organization Code

7. Author(s)	8. Performing Organization Report No.
Richard Eppler Dan M. Somers	

9 Performing Organization Name and Address	10. Work Unit No.
NASA Langley Research Center Hampton, VA 23665	505-31-33-05
	11. Contract or Grant No.

12. Sponsoring Agency Name and Address	13. Type of Report and Period Covered
National Aeronautics and Space Administration Washington, DC 20546	Technical Memorandum
	14. Sponsoring Agency Code

15. Supplementary Notes

Richard Eppler: Professor, University of Stuttgart, Stuttgart, West Germany.
Dan M. Somers: Langley Research Center.
This report supplements NASA TM-80210.

16. Abstract

Three new options have been incorporated into an existing computer program for the design and analysis of low-speed airfoils. These options permit the analysis of airfoils having variable chord (variable geometry), a boundary-layer displacement iteration, and the analysis of the effect of single roughness elements. All three options are described in detail and are included in the FORTRAN IV computer program which is available through COSMIC.

17. Key Words (Suggested by Author(s))	18. Distribution Statement
Airfoils Low speed Panel methods Boundary-layer methods	Unclassified - Unlimited Subject Category 02

19. Security Classif. (of this report)	20. Security Classif. (of this page)	21. No. of Pages	22. Price*
Unclassified	Unclassified	28	A03

* For sale by the National Technical Information Service, Springfield, Virginia 22161

SUPPLEMENT TO: A COMPUTER PROGRAM FOR THE DESIGN AND ANALYSIS OF LOW-SPEED AIRFOILS

Richard Eppler* and Dan M. Somers
Langley Research Center

SUMMARY

Three new options have been incorporated into an existing computer program for the design and analysis of low-speed airfoils. These options permit the analysis of airfoils having variable chord (variable geometry), a boundary-layer displacement iteration, and the analysis of the effect of single roughness elements. All three options are described in detail and are included in the FORTRAN IV computer program which is available through COSMIC.

INTRODUCTION

A conformal-mapping method for the design of airfoils with prescribed velocity-distribution characteristics, a panel method for the analysis of the potential flow about given airfoils, and a boundary-layer method have been combined. With this combined method, airfoils with prescribed boundary-layer characteristics can be designed and airfoils with prescribed shapes can be analyzed. All three methods and the FORTRAN IV computer program for the numerical evaluation of these methods are described in reference 1.

Three new options have been incorporated into the computer program described in reference 1. The previous version of the program (ref. 1) was capable of analyzing an airfoil with a simple flap. In the present version, an option has been added which allows the analysis of an airfoil having variable chord (variable geometry). The method of reference 1 did not contain a boundary-layer displacement iteration. An iteration procedure has been included in the present version. The third option to be added permits the analysis of the effect of single roughness elements. The input for all three options is described in detail.

Use of trade names or names of manufacturers in this report does not constitute an official endorsement of such products or manufacturers, either expressed or implied, by the National Aeronautics and Space Administration.

---

*Professor, University of Stuttgart, Stuttgart, West Germany.

SYMBOLS

Values are given in SI units.

C_f	boundary-layer skin-friction coefficient
c	airfoil chord, m
c_d	section profile-drag coefficient
c_l	section lift coefficient
c_m	section pitching-moment coefficient about quarter-chord point
h	height of roughness element normal to surface, m
ls	lower surface
R	Reynolds number based on free-stream conditions and airfoil chord
R_h	Reynolds number based on local conditions and height of roughness element
U	potential-flow velocity, m/s
U_∞	free-stream velocity, m/s
u_h	x-component of velocity in turbulent boundary-layer at height of roughness element, m/s
us	upper surface
v	local velocity on airfoil, m/s
x	airfoil abscissa, m; axis in streamwise direction, tangential to surface
x_R	chord location of roughness element, m
y	airfoil ordinate, m
α	angle of attack relative to zero-lift line, deg
Δ	incremental change in quantity
δ_1	boundary-layer displacement thickness, m
δ_2	boundary-layer momentum thickness, m
ν	kinematic viscosity, m^2/s

ρ air density, kg/m^3

τ_0 shear stress at wall, $kg/m \cdot s^2$

PROGRAM AVAILABILITY

The program is available at a nominal fee through the following organization:

Computer Software Management Information Center (COSMIC)
112 Barrow Hall, University of Georgia
Athens, Georgia 30602

Request the program by the designation PROFILE LAR-12727.

VARIABLE GEOMETRY

The previous version of the computer program (ref. 1) allowed the shape of an airfoil analyzed by the panel method to be altered so as to correspond to the deflection of a simple flap. Thus, that version only permitted the rotation of a portion of the airfoil, the flap, about a specified hinge point. Chord-increasing flaps were not allowed. The present version of the program can analyze this form of variable geometry. It should be noted that, while the airfoil shape which results from the exercise of this option does have an increased chord, it does not contain a slot and, thus, is still a single-element as opposed to a multi-element airfoil. An application of this capability is described in reference 2.

FLAP Card

The variable-geometry option is selected by setting NUPU = 1, 2, 3, or 4 on the FLAP card.

NUPA, NUPE, and NUPI are neglected.

NUPU = 1 — The F-words specify the points to be deleted. The five digits of F_i are denoted aaabb. Points aaa through aaa + bb are deleted. If bb = 00, only point aaa is deleted.

It is recommended that the F-words be specified with decreasing values of aaa as the points after point aaa (higher point number) are renumbered. This means that aaa for F_1 should be greater than aaa for F_2 which should be greater than aaa for F_3 and so on.

Only one FLAP card with NUPU = 1 is allowed.

NUPU = 2 - The F-words specify points to be added to the upper surface. The new points are added after the point on the upper surface having the greatest x/c remaining after the deletions which resulted from the FLAP card with NUPU = 1. Thus, if point 1 (x/c = 1) was not deleted, only points with x/c > 1 can be added.

$0.01F_1 = x_1/c$ [F5.4]

$0.01F_2 = y_1/c$ [F5.4]

$(F_3,F_4) = (x_2/c,y_2/c)$ and so on

It should be noted that the new points must be in order of increasing x/c.

NUPU = 3 – The F-words specify points to be added to the lower surface. The F-words are interpreted just as they are for a FLAP card with NUPU = 2.

NUPU = 4 – The F-words specify additional points to be splined in between the points available so far. The F-words are interpreted just as they are for an FXPR card. (See ref. 1, p. 45.)

It should be remembered that the points are renumbered during the execution of each of the preceding FLAP cards.

The panel method is called automatically after a FLAP card with NUPU = 4 is read. Following this card, any other cards (in the proper sequence, of course) are allowed except another FLAP card. Only airfoil coordinates generated in the design mode or read in following an FXPR card can be altered by FLAP cards with NUPU = 1, 2, 3, and 4. Thus, a FLAP card with NUPU = 1, 2, 3, or 4 cannot follow another FLAP card.

Example

The following card sequence illustrates the use of the variable-geometry option.

```
TRA1   664 1250  400 1450  000 1650  300 1850  400 2050  500 2250  600 2450  700
TRA1   664 2650  900 2940  900 3030 1020  000 1300 3350  100 3550  200 4350  300
TRA1   664 4550  200 4750  100 4950  000 5150 2500 6000  400
TRA2   664  400 1250  200 1000  720  400  850  200  900  710  100  300  000  000
ALFA  1  1  000
DIAG     1
FLAP     1 5209  700  500  201
FLAP     211000 -35012000 -900
FLAP     3 8400 -265 9600 -29010200 -49012000 -900
FLAP     45240051200502004920002200013000
ALFA  1  1  000
DIAG     2
ENDE
```

The first FLAP card deletes points 52 through 61 as well as points 7, 5, 3, and 2 (in the x-y-v listing, N = 51 through 60, 6, 4, 2, and 1). If the chord is to be increased, some of the points near the trailing edge should be deleted. In other words, a short distance between points is required near the new trailing edge, not the old one. The second FLAP card specifies two points for the extension of the upper surface: (x/c = 1.1000,y/c = -0.0350) and (x/c = 1.2000,y/c = -0.0900). The third FLAP card specifies four points for the extension of the lower surface: (x/c = 0.8400,y/c = -0.0265), (x/c = 0.9600,y/c = -0.0290), (x/c = 1.0800,y/c = -0.0490), and (x/c = 1.2000,y/c = -0.0900). The fourth FLAP card inserts in the equiangular-spacing mode (ref. 1) four points between points 52 and 53, two points between points 51 and 52, two points between points 50 and 51, two points between points 49 and 50, two points between points 2 and 3, and three points between points 1 and 2. The panel method is called automatically after the fourth FLAP card.

This card sequence plots into one diagram (fig. 1) the velocity distributions for airfoil 664 with and without the variable-geometry flap extension. Two velocity distributions, each at $\alpha = 0^{0}$ relative to the chord line, are plotted. The following x-y-v listings are also generated.

AIRFOIL 664 16.63% 0.00

N	X	Y	VELOCITY DISTRIBUTIONS FOR THE ABOVE ANGLES OF ATTACK RELATIVE TO THE CHORD LINE
0	1.00000	0.00000	.773
1	.99623	.00092	.799
2	.98557	.00391	.862
3	.96923	.00881	.934
4	.94774	.01491	.978
5	.92110	.02193	.997
6	.88964	.03005	1.020
7	.85407	.03927	1.048
8	.81512	.04942	1.081
9	.77353	.06020	1.121
10	.73008	.07122	1.167
11	.68549	.08197	1.220
12	.64043	.09167	1.281
13	.59497	.09937	1.318
14	.54869	.10482	1.326
15	.50167	.10840	1.331
16	.45437	.11029	1.334
17	.40727	.11060	1.335
18	.36097	.10939	1.335
19	.31564	.10670	1.334
20	.27205	.10262	1.330
21	.23051	.09720	1.324
22	.19145	.09055	1.315
23	.15521	.08277	1.301
24	.12216	.07401	1.281
25	.09258	.06441	1.252
26	.06674	.05416	1.211
27	.04487	.04348	1.150
28	.02714	.03261	1.058
29	.01371	.02183	.909
30	.00468	.01155	.661
31	.00023	.00229	.197
32	.00146	-.00521	.562
33	.00903	-.01173	.842
34	.02234	-.01817	.954
35	.04097	-.02423	1.004
36	.06471	-.02979	1.028
37	.09334	-.03482	1.039
38	.12651	-.03936	1.046
39	.16380	-.04341	1.052
40	.20474	-.04693	1.057
41	.24882	-.04990	1.060
42	.29552	-.05229	1.064
43	.34429	-.05406	1.066

```
AIRFOIL  664    16.63%      0.00
  N        X         Y      VELOCITY DISTRIBUTIONS FOR THE ABOVE ANGLES OF ATTACK RELATIVE TO THE CHORD LINE
 44     .39452   -.05522    1.070
 45     .44556   -.05572    1.074
 46     .49678   -.05546    1.079
 47     .54754   -.05433    1.084
 48     .59719   -.05219    1.090
 49     .64512   -.04967    1.096
 50     .69117   -.04322    1.076
 51     .73561   -.03567    1.036
 52     .77909   -.02623     .957
 53     .82219   -.01637     .875
 54     .86399   -.00803     .823
 55     .90260   -.00224     .787
 56     .93641    .00102     .761
 57     .96395    .00198     .751
 58     .98400    .00142     .757
 59     .99602    .00045     .767
 60    1.00000   -.00000     .773
ALPHAO = 3.85 DEGREES   CMO = -.0909   ETA = 1.131

VARIABLE GEOMETRY AIRFOIL  664
 DELETED POINTS 52 THROUGH 61
 DELETED POINT   7
 DELETED POINT   5
 DELETED POINTS  2 THROUGH  3
 INSERTED POINT ON UPPER SURFACE AT   X/C = 1.1000   Y/C = -.0350
 INSERTED POINT ON UPPER SURFACE AT   X/C = 1.2000   Y/C = -.0900
 INSERTED POINT ON LOWER SURFACE AT   X/C =  .8400   Y/C = -.0265
 INSERTED POINT ON LOWER SURFACE AT   X/C =  .9600   Y/C = -.0290
 INSERTED POINT ON LOWER SURFACE AT   X/C = 1.0800   Y/C = -.0490
 INSERTED POINT ON LOWER SURFACE AT   X/C = 1.2000   Y/C = -.0900
```

PANEL METHOD AIRFOIL 664 CA = 1.58921, 6.78770 ALPHAD =13.18 DEGREES
AIRFOIL 664 16.63% THICKNESS 0.00% FLAP 0.00 DEGREES DEFLECTION
0.00

N	X	Y	VELOCITY DISTRIBUTIONS FOR THE ABOVE ANGLES OF ATTACK RELATIVE TO THE CHORD LINE
0	1.20000	-.09000	.819
1	1.19373	-.08620	.920
2	1.17500	-.07496	1.021
3	1.14391	-.05709	1.137
4	1.10000	-.03500	1.261
5	1.07054	-.02294	1.290
6	1.03709	-.01132	1.294
7	1.00000	0.00000	1.285
8	.96923	.00381	1.286
9	.92110	.02193	1.294
10	.85407	.03927	1.303
11	.81512	.04942	1.326
12	.77353	.06020	1.359
13	.73008	.07122	1.401
14	.68549	.08197	1.455
15	.64043	.09167	1.516
16	.59497	.09937	1.554
17	.54869	.10482	1.563
18	.50167	.10840	1.568
19	.45437	.11029	1.572
20	.40727	.11060	1.577
21	.36097	.10938	1.562
22	.31564	.10670	1.589
23	.27205	.10262	1.596
24	.23051	.09720	1.605
25	.19145	.09055	1.614
26	.15521	.08277	1.623
27	.12216	.07401	1.633
28	.09258	.06441	1.643
29	.06674	.05416	1.652
30	.04487	.04348	1.661
31	.02714	.03261	1.663
32	.01371	.02183	1.661
33	.00468	.01155	1.612
34	.00023	.00229	1.553
35	.00146	-.00521	.868
36	.00903	-.01173	.072
37	.02234	-.01817	.283
38	.04097	-.02423	.479
39	.06471	-.02979	.597
40	.09334	-.03482	.671
41	.12651	-.03936	.722

AIRFOIL 664 16.63% THICKNESS 0.00% FLAP 0.00 DEGREES DEFLECTION

0.00

N	X	Y	VELOCITY DISTRIBUTIONS FOR THE ABOVE ANGLES OF ATTACK RELATIVE TO THE CHORD LINE
42	.16380	-.04341	.759
43	.20474	-.04693	.787
44	.24582	-.04990	.808
45	.29552	-.05229	.824
46	.34429	-.05406	.835
47	.39452	-.05522	.844
48	.44556	-.05572	.850
49	.49678	-.05546	.855
50	.54754	-.05433	.856
51	.59719	-.05219	.854
52	.64512	-.04867	.946
53	.69117	-.04322	.801
54	.74184	-.03641	.747
55	.79152	-.03041	.700
56	.84000	-.02650	.666
57	.88180	-.02542	.653
58	.92188	-.02639	.646
59	.96000	-.02900	.647
60	1.00411	-.03401	.644
61	1.04421	-.04078	.647
62	1.08000	-.04900	.660
63	1.12280	-.06177	.698
64	1.15631	-.07351	.736
65	1.18047	-.08254	.757
66	1.19510	-.08812	.774
67	1.20000	-.09000	.819

BOUNDARY-LAYER DISPLACEMENT ITERATION

The theoretical results for c_l versus c_d from the previous version of the computer program (ref. 1) agree remarkably well with experimental measurements. (For example, see ref. 3.) This good agreement, however, does not hold for c_l versus α or c_m versus α, particularly for aft-loaded airfoils. This is not surprising in that the boundary-layer displacement effect was only accounted for by reducing the lift-curve slope from its theoretical value to 2π. An improvement could therefore be expected from a more detailed analysis of the displacement effect.

There exists, however, a fundamental flaw in the philosophy of the application of displacement iterations. All displacement effects are of second order in boundary-layer theory (ref. 4). Accordingly, it is inconsistent to include the displacement effect while neglecting other pertinent second-order effects which arise from the pressure gradient normal to the surface within the boundary layer and other y-component terms in the Navier-Stokes equations. This flaw becomes more significant as the boundary-layer thickness increases.

At the trailing edge, difficult problems arise. The potential-flow solution yields steep pressure gradients toward the trailing edge which result in a very high slope for the displacement thickness. This high slope can result in a rapid divergence for the displacement iteration, even for high Reynolds numbers. The order (quality) of the trailing-edge treatment has a significant influence on the results. The wake solution incorporated in the present panel method gives very precise results for the lift coefficients of airfoils with blunt trailing edges. It, however, also predicts steep pressure gradients toward the trailing edge which, in turn, accelerate the divergence of the displacement iteration. Moreover, this solution also clearly shows that the small region which surrounds the trailing edge has a great influence on the solution for the entire airfoil.

One solution to this divergence problem is to artificially smooth the boundary-layer displacement after each iteration. But, even if convergence is obtained and, furthermore, even if smoothing were not required for convergence, the iteration process would still be questionable due to the neglect of the second-order boundary-layer terms previously mentioned. A wake solution which minimizes the pressure gradients near the trailing edge could improve the iteration process but would not eliminate the fundamental flaw in philosophy.

The question remains as to what simple procedures can be developed to obtain at least a rough estimate of the displacement effect. As previously explained, multiple iterations are not logical. Accordingly, in the present method, only one iteration is performed. The displacement thickness is smoothed once and then added to the airfoil contour. The lift and pitching-moment coefficients are then computed for the new contour and stored. Later the linear portions of the $c_l - \alpha$ and $c_m - \alpha$ curves are adjusted by a least-squares fit to these stored values. The separation corrections are then applied as discussed in reference 1. Thus, only a few angles of attack require this displacement iteration. The remaining angles of attack are adjusted according to the least-squares fit. The displacement effect is considered to be linear in α. A higher-order effect cannot be expected from such a simple approach.

This simple procedure does not require much computing time. The results, of course, depend on the smoothing process. In the present version of the program, the curvature of $\delta_1(x)$ $\left(\text{i.e., } \frac{d^2\delta_1}{dx^2}\right)$ is limited. The limit can be specified in the input. This limit (SLM) is preset to $\frac{1}{2}\frac{d^2\delta_1}{dx^2} < 0.5$ ($\equiv$ SLM).

The single iteration is initiated by one input card, which must immediately precede an input card which initiates a boundary-layer computation (i.e., an RE , FLZW, or PLW card).

DPIT Card

NUPA, NUPE, NUPI, and NUPU are neglected.

The F-words specify the angles of attack for which a displacement iteration is performed and also the plot mode mbt. The five digits of F_i are denoted abcde. The variable abc is interpreted as an integer n and a displacement iteration is initiated for the nth angle of attack on the preceding ALFA card. A displacement iteration is performed for each Reynolds number from the immediately following RE , FLZW, or PLW card. The variable d determines the plot mode. If $d > 0$, a diagram containing the airfoil contour (including the displacement thickness) and the velocity distribution for the angle of attack under consideration is plotted after each displacement iteration. The plot mode mbt is set equal to $d - 1$ and is described under "DIAG Card" in reference 1 (p. 52) and reviewed below.

$d = 1$ — Axes are drawn, one set of data is plotted, and the diagram is terminated (i.e., closed to further plotting).

$d = 2$ — Axes are drawn, one set of data is plotted, and the diagram is open to further plotting.

d = 3 — No axes are drawn and one set of data is plotted into the existing diagram which is then terminated.

d = 4 — No axes are drawn and one set of data is plotted into the existing diagram which remains open to further plotting.

If d = 2 or 3, the RE , FLZW, or PLW card must specify only one Reynolds number.

Up to five F-words are allowed which means that displacement iterations can be performed for up to five angles of attack.

If $F_5 < 0$, the limit for $\frac{d^2\delta_1}{dx^2}$ is set to SLM = -0.bcde. This new limit is used until it is reset by another DPIT card with $F_5 < 0$. Obviously, only four angles of attack can be specified on DPIT cards with $F_5 < 0$.

Examples

The following card sequences illustrate some of the DPIT-card options.

```
TRA1  0315 1650  400 1750  100 1850  400 2050  410 2250  430 2450  470 2650  550
TRA1  0315 2850  710 3050 1030  000 1670 3250   30 3450   70 3650   90 3850  100
TRA1  0315 4050   85 4250   55 4450  -05 4650 -135 4850 -265 6000  100
TRA2  0315  400 1650  200  400  770  600 1150  200  300  650  300  300  000  000
ALFA    10  000  100  200  300  400  500  600  700  800  900
DIAG
DPIT        110  510  910
RE        03    200003    6000
CDCL
ENDE
```

After the RE card is read, displacement iterations for the first, fifth, and ninth angles of attack (i.e., $\alpha = 0^0$, 4^0, and 8^0 relative to the zero-lift line) are performed for both $R = 2 \times 10^6$ and $R = 6 \times 10^6$. A diagram is plotted for each displacement iteration. A potential-flow diagram (no displacement iteration) is also plotted (DIAG card). Thus, one diagram containing 10 velocity distributions (DIAG card) (fig. 2) and six diagrams containing one velocity distribution each (DPIT card) (fig. 3) are plotted. The $c_l - \alpha$ and $c_m - \alpha$ portions of the boundary-layer summary and its plot (CDCL card) are adjusted according to the computed displacement effect.

It should be noted that each displacement iteration requires a solution from the panel method. Thus, for an airfoil having 61 points, each displacement iteration requires approximately 8 seconds CPU time on a Control Data 6600 computer.

```
TRA1  0215 1650  400 1750  100 1850  400 2050  410 2250  430 2450  470 2650  550
TRA1  0215 2950  710 3050 1030  000 1670 3250   30 3450   70 3650   90 3850  100
TRA1  0315 4050   35 4250   55 4450  -05 4650 -125 4950 -365 6000  100
TRA2  0315  400 1650  200  400  770  600 1150  200  300  650  300  300  000  000
ALFA     2  300  700
DIAG     1
ALFA    10  000  100  200  300  400  500  600  700  800  900
DPIT         440  930
RE          03    6000
CDCL
ENDE
```

The preceding card sequence plots one diagram (fig. 4) which contains both potential-flow and displacement-iteration shapes and velocity distributions for $\alpha = 3^0$ and 7^0. Note that only one Reynolds number is considered and that displacement iterations are only performed for $\alpha = 3^0$ and 7^0. The boundary-layer summary which follows contains the adjustments due to the computed displacement effect. AC is the adjusted angle of attack (relative to the zero-lift line).

SUMMARY AIRFOIL 315 ANGLE OF ATTACK RELATIVE TO THE ZERO-LIFT LINE ALPHAO = 2.95 DEGREES
* INDICATES VELOCITY REDUCTION WITHIN BUBBLE BELOW .94

R = 6000000 MU = 3

ALPHA = 0.00 DEGREES

	1 S TURB	S SEP	CD
UPPER	.5749	0.0000	.0030
LOWER	.4107	0.0000	.0017
TOTAL	CL = 0.000	CD =	.0047
	CM = -.0662	AC =	.18

ALPHA = 1.00 DEGREES

	1 S TURB	S SEP	CD
UPPER	.5676	0.0000	.0032
LOWER	.4086	0.0000	.0016
TOTAL	CL = .110	CD =	.0048
	CM = -.0682	AC =	1.11

ALPHA = 2.00 DEGREES

	1 S TURB	S SEP	CD
UPPER	.5980	0.0000	.0034
LOWER	.4069	0.0000	.0015
TOTAL	CL = .220	CD =	.0049
	CM = -.0702	AC =	2.05

ALPHA = 3.00 DEGREES

	1 S TURB	S SEP	CD
UPPER	.6067	0.0000	.0036
LOWER	.4052	0.0000	.0015
TOTAL	CL = .330	CD =	.0050
	CM = -.0722	AC =	2.98

ALPHA = 4.00 DEGREES

	1 S TURB	S SEP	CD
UPPER	.6147	0.0000	.0038
LOWER	.4036	0.0000	.0014
TOTAL	CL = .440	CD =	.0052
	CM = -.0742	AC =	3.91

ALPHA = 5.00 DEGREES

	1 S TURB	S SEP	CD
UPPER	.6569	0.0000	.0042
LOWER	.4022	0.0000	.0013
TOTAL	CL = .550	CD =	.0056
	CM = -.0762	AC =	4.85

SUMMARY AIRFOIL 315 ANGLE OF ATTACK RELATIVE TO THE ZERO-LIFT LINE ALPHA0 = 2.95 DEGREES
* INDICATES VELOCITY REDUCTION WITHIN BUBBLE BELOW .94

R = 6000000 MU = 3

ALPHA = 6.00 DEGREES

	1 S TURB	S SEP	CD
UPPER	.7525	0.0000	.0051
LOWER	.4007	0.0000	.0013
TOTAL	CL = .660	CD = .0064	
	CM = -.0782	AC = 5.78	

ALPHA = 7.00 DEGREES

	1 S TURB	S SEP	CD
UPPER	.8430	.0006	.0063
LOWER	.3992	0.0000	.0012
TOTAL	CL = .769	CD = .0075	
	CM = -.0801	AC = 6.71	

ALPHA = 8.00 DEGREES

	1 S TURB	S SEP	CD
UPPER	.9073	.0036	.0074
LOWER	.3978	0.0000	.0012
TOTAL	CL = .876	CD = .0086	
	CM = -.0813	AC = 7.64	

ALPHA = 9.00 DEGREES

	1 S TURB	S SEP	CD
UPPER	.9467	.0071	.0085
LOWER	.3962	0.0000	.0011
TOTAL	CL = .982	CD = .0096	
	CM = -.0823	AC = 8.58	

SINGLE ROUGHNESS ELEMENTS

Recent flight and wind-tunnel experiments indicate that single roughness elements such as flap and aileron hinges and poorly faired spoilers significantly degrade the overall performance of an airplane (ref. 5). With the previous version of the program (ref. 1), only the effect of roughness on boundary-layer transition could be considered. Fixed transition points could be specified using transition mode 1 or 2, whereas premature transition due to distributed roughness or free-stream turbulence could be analyzed using transition modes greater than 3. (See "RE Card," ref. 1, p. 56.)

In the present version of the program, an option has been added which allows the analysis of the effect of single roughness elements on a turbulent as well as a laminar boundary layer. The method is described in detail in reference 5 and reviewed below.

The increase $\Delta\delta_2$ of the boundary-layer momentum thickness δ_2 due to a single roughness element of height h is assumed to depend only on the local roughness Reynolds number $R_h = \frac{u_h h}{\nu}$ where u_h is the x-component of the velocity in the turbulent boundary layer at a distance h from the surface. For a turbulent boundary layer, the increase of δ_2 due to the roughness element is assumed to be

$$\frac{\Delta\delta_2}{c} = 0.15 \frac{u_h}{U_\infty} \frac{h}{c}$$

where c is the airfoil chord and U_∞ is the free-stream velocity. An expression for the velocity u_h is taken from reference 6 and transformed to the variables available in the boundary-layer method. This yields

$$\frac{u_h}{U} = \sqrt{c_f} \left[2.17 \ln\left(\sqrt{c_f} \frac{U}{U_\infty} R \frac{h}{c} \right) + 6.5 \right]$$

where U is the local potential-flow velocity, $c_f \left(= \frac{\tau_0}{\rho U^2} \right)$ is the local skin-friction coefficient, and $R \left(= \frac{U_\infty c}{\nu} \right)$ is the Reynolds number based on free-stream conditions and airfoil chord. In the skin-friction coefficient, τ_0 is the shear stress at the wall and ρ is the air density.

If the boundary layer is laminar at the position of the roughness element, transition is assumed to occur at that position. This is specified as $h = 0$ which acts as a "latest" transition point. Upstream of that position, any transition mode except 1 or 2 (fixed transition) is allowed. This approach is more logical for many analyses than fixed transition, in front of which no other transition criterion is applied except transition following laminar separation. Fixed transition (mode 1 or 2) alone could result in delayed transition at some (high) angles of attack - an effect which is obviously not intended.

RE Card

F-words 11-14 contain the data for single roughness elements. These words previously only contained the transition points for transition modes 1 and 2 (fixed transition).

If $F_{14} < 0$, F-words 11-14 specify single roughness elements and, therefore, transition modes 1 and 2 cannot be used. The five digits of F_{11} - F_{14} are denoted abbcc. For F_{11} - F_{13}, a is either a blank or 0. For F_{14}, a is a minus sign (-). The digits bb specify the location of the roughness element x_R in percent chord. The digits cc which are read as 0.cc specify the roughness height h in percent chord. Thus, roughness heights can be specified over the range $0.0001 \leq h/c \leq 0.0099$. F_{11} and F_{12} specify roughness elements on the upper surface whereas F_{13} and F_{14} are for the lower surface. If $x_R = 0$ is specified, no roughness element is introduced for that F-word. Thus, 0, 1, or 2 roughness elements can be specified on each surface.

F_{11} - F_{14} are read from each RE card which specifies at least one Reynolds number. The roughness elements remain in effect until an RE card with $F_2 \neq 0$ is read.

Roughness elements can only be analyzed at positions which are actual airfoil coordinates. If x_R is specified at an x/c which does not correspond to any of the airfoil coordinates, the roughness-element location is shifted to the next airfoil coordinate downstream of x_R. If there is no airfoil coordinate close enough to the desired roughness-element location, one can be inserted using a PAN or FXPR card. (See ref. 1.)

Examples

The following RE card specifies two roughness elements on the upper surface at $x/c = 0.60$ and $x/c = 0.80$, each with a height $h/c = 0.0010$, and one roughness element on the lower surface at $x/c = 0.70$, with a height $h/c = 0.0015$.

```
RE        03    4000                                    6010 8010 0000-7015
```

The following RE card specifies the same roughness elements on the upper surface and none on the lower surface.

```
RE        03    4000                                        6010 8010 0000-0001
```

REFERENCES

1. Eppler, Richard; and Somers, Dan M.: A Computer Program for the Design and Analysis of Low-Speed Airfoils. NASA TM-80210, 1980.

2. Eppler, Richard: Some New Airfoils. Science and Technology of Low Speed and Motorless Flight, NASA CP-2085, Part 1, 1979, pp. 131-153.

3. Eppler, Richard; and Somers, Dan M.: Low Speed Airfoil Design and Analysis. Advanced Technology Airfoil Research - Volume I, NASA CP-2045, Part 1, 1979, pp. 73-99.

4. Van Dyke, Milton: Perturbation Methods in Fluid Mechanics. Applied Mathematics and Mechanics, F. N. Frenkiel and G. Temple, eds., Academic Press, Inc., 1964, pp. 132-134.

5. Eppler, Richard: The Effect of Disturbances on a Wing. Science and Technology of Low Speed and Motorless Flight, NASA CP-2085, Part 1, 1979, pp. 81-91.

6. Ludwieg, H.; and Tillman, W.: Investigations of the Wall-Shearing Stress in Turbulent Boundary Layers. Ingenieur-Archiv, vol. 17, no. 4, 1949, pp. 288-299.

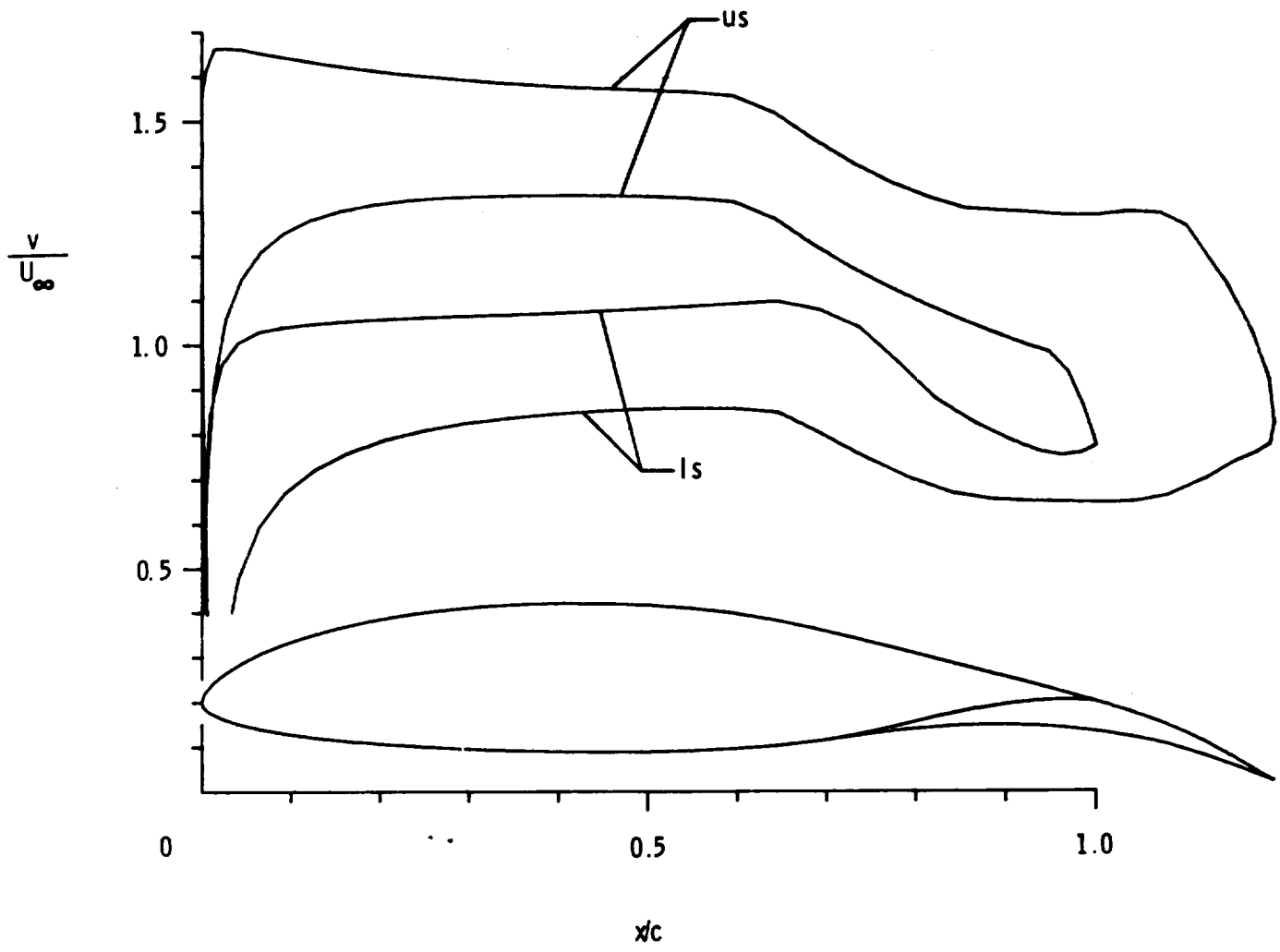

Figure 1.- Variable geometry. (Airfoil 664; $\alpha = 0^0$ relative to chord line)

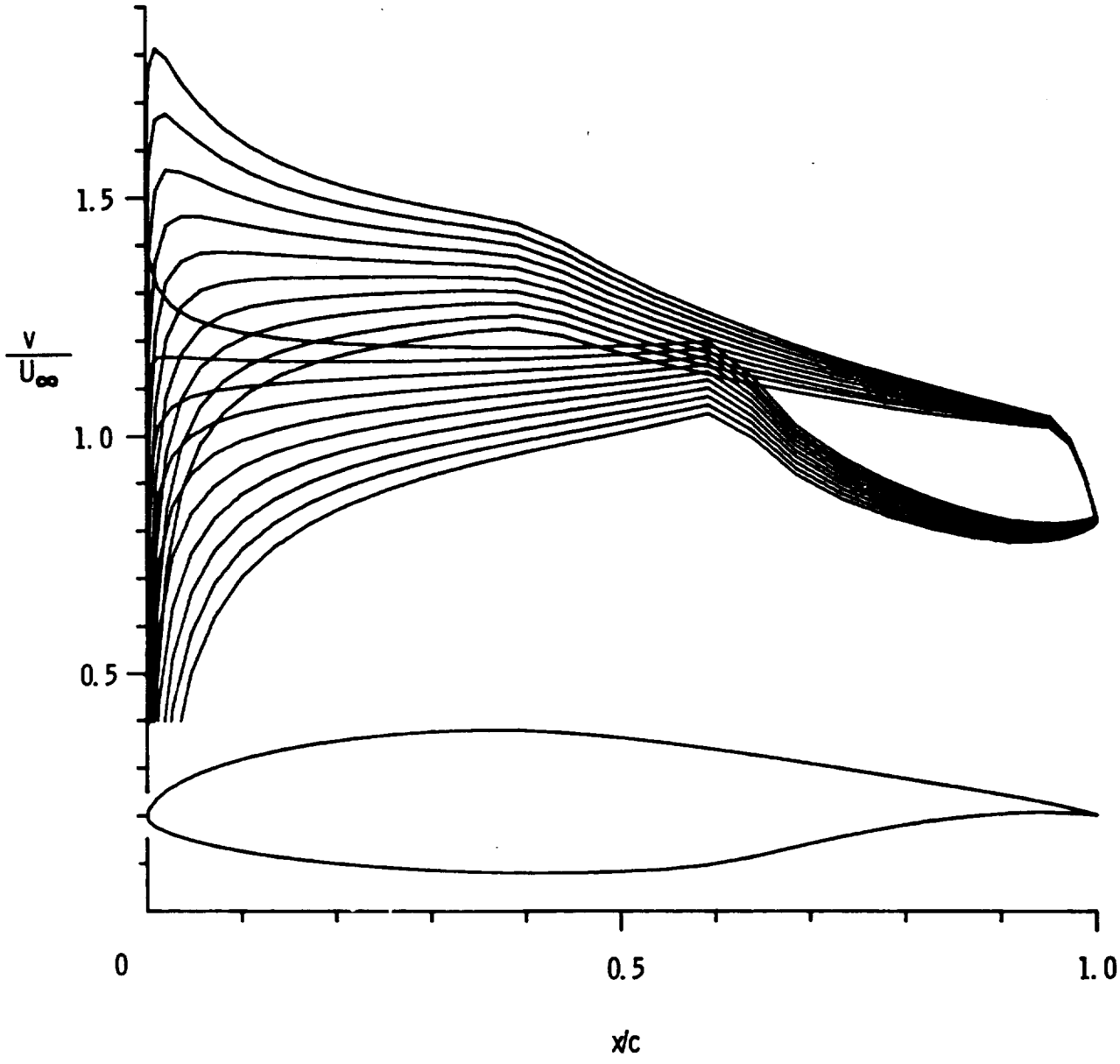

Figure 2. - Diagram without boundary-layer displacement iteration.
($\alpha = 0^0 - 9^0$ relative to zero-lift line)

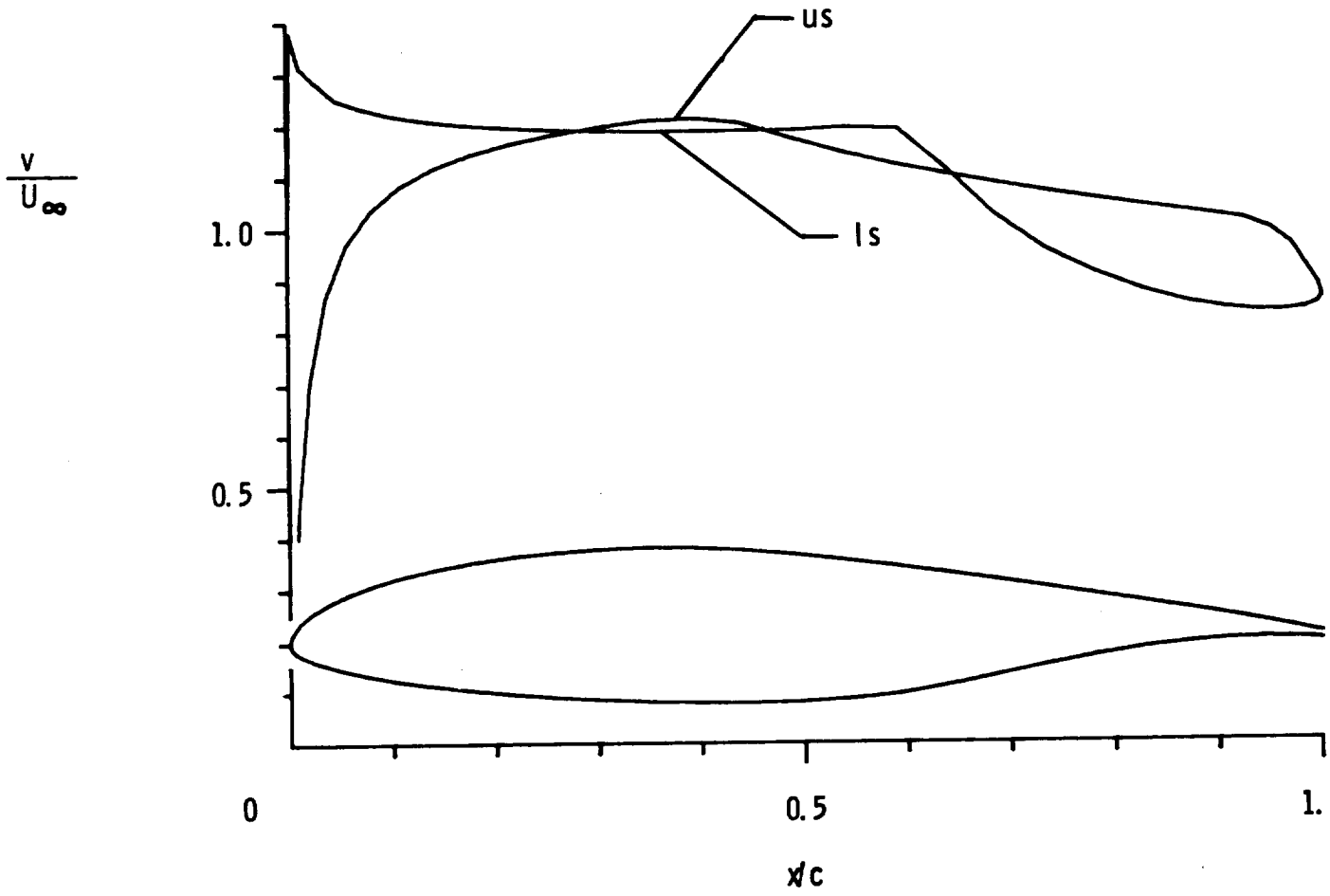

(a) $\alpha = 0^0$; $R = 2 \times 10^6$.

Figure 3. - Diagram with boundary-layer displacement iteration.
(α relative to zero-lift line)

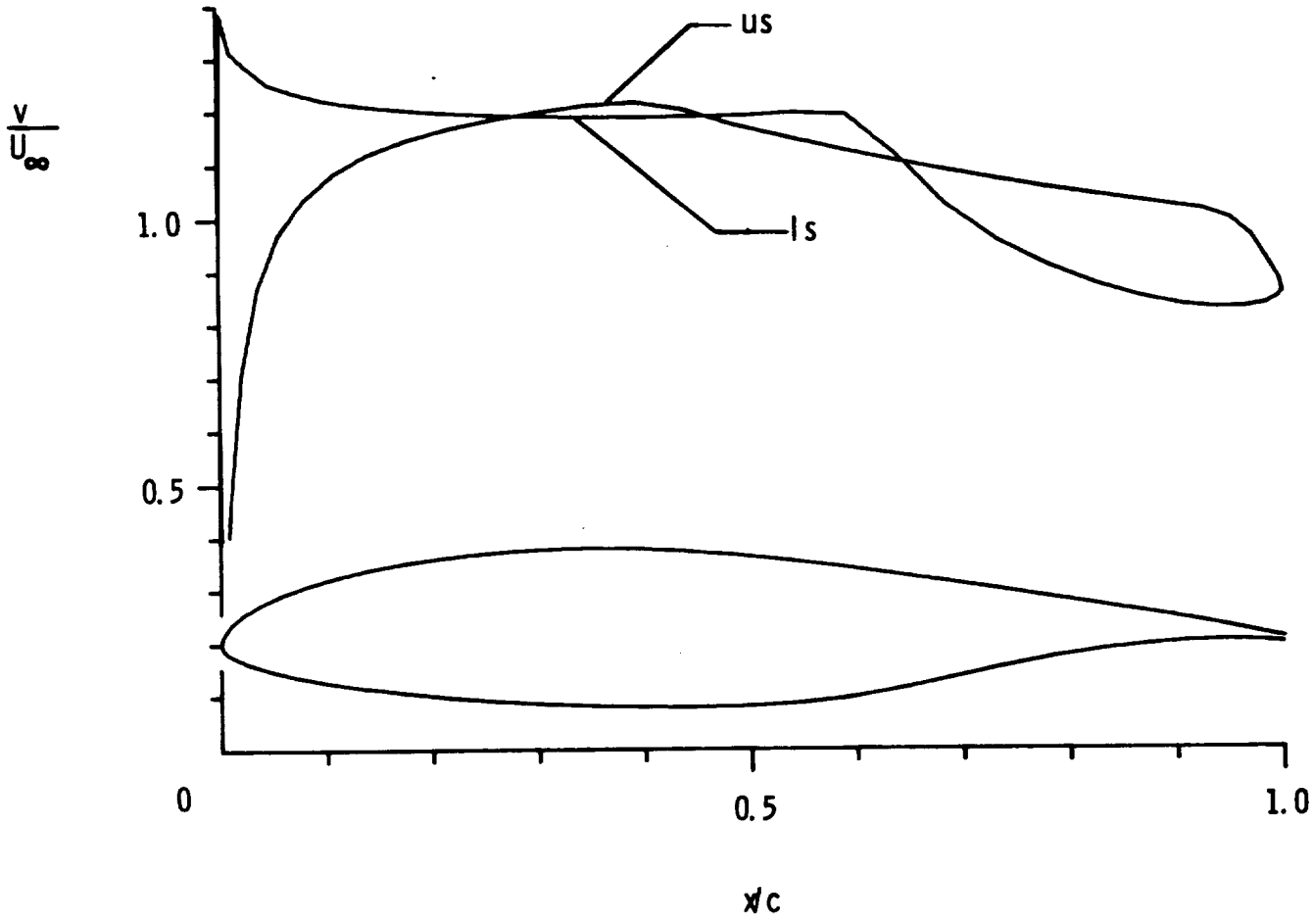

(b) $\alpha = 0^{o}$; $R = 6 \times 10^{6}$.

Figure 3. - Continued.

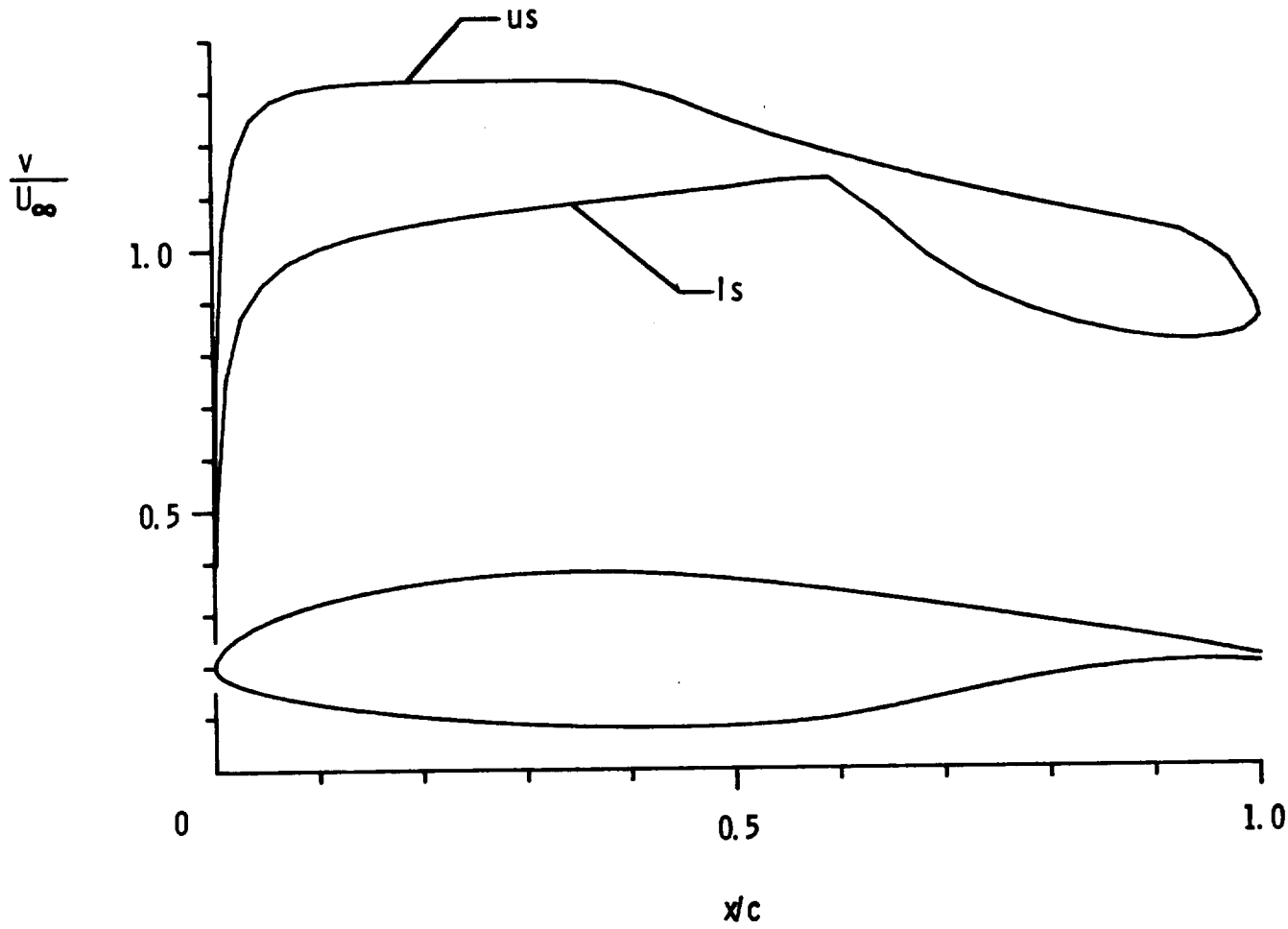

(c) $\alpha = 4^0$; $R = 2 \times 10^6$.

Figure 3. - Continued.

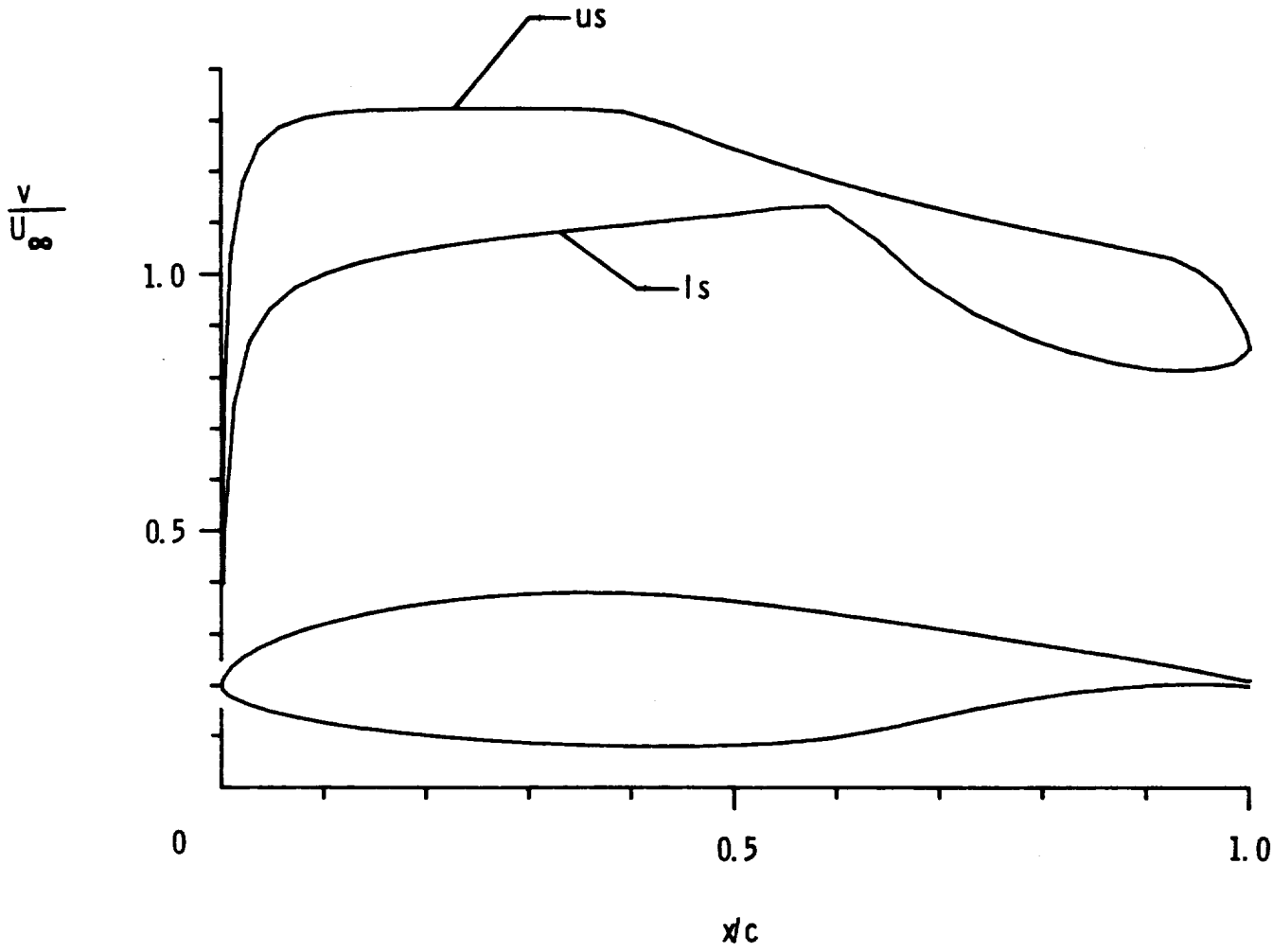

(d) $\alpha = 4^0$; $R = 6 \times 10^6$.

Figure 3. - Continued.

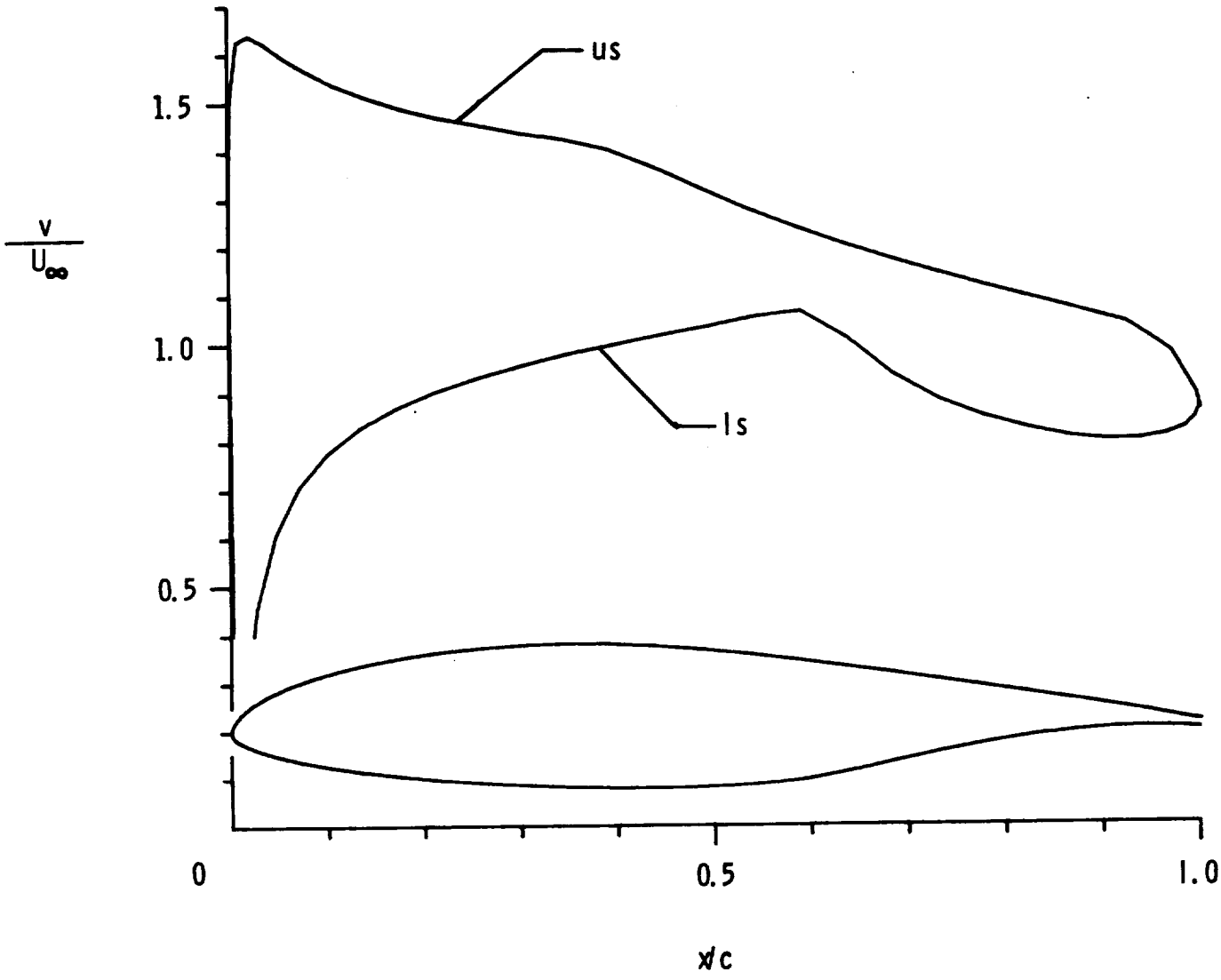

(e) $\alpha = 8^0$; $R = 2 \times 10^6$.

Figure 3. - Continued.

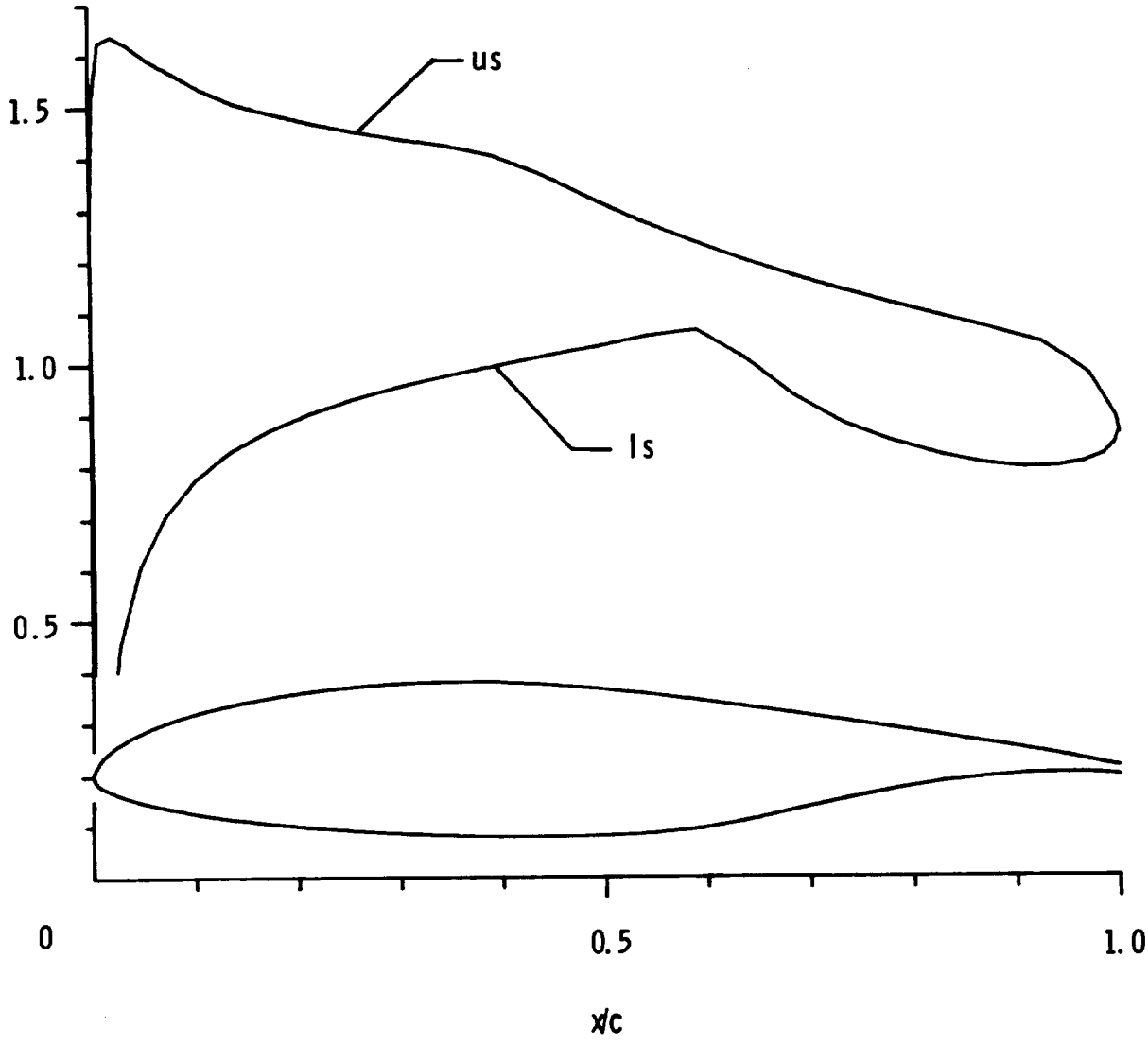

(f) $\alpha = 8^0$; $R = 6 \times 10^6$.

Figure 3. - Concluded.

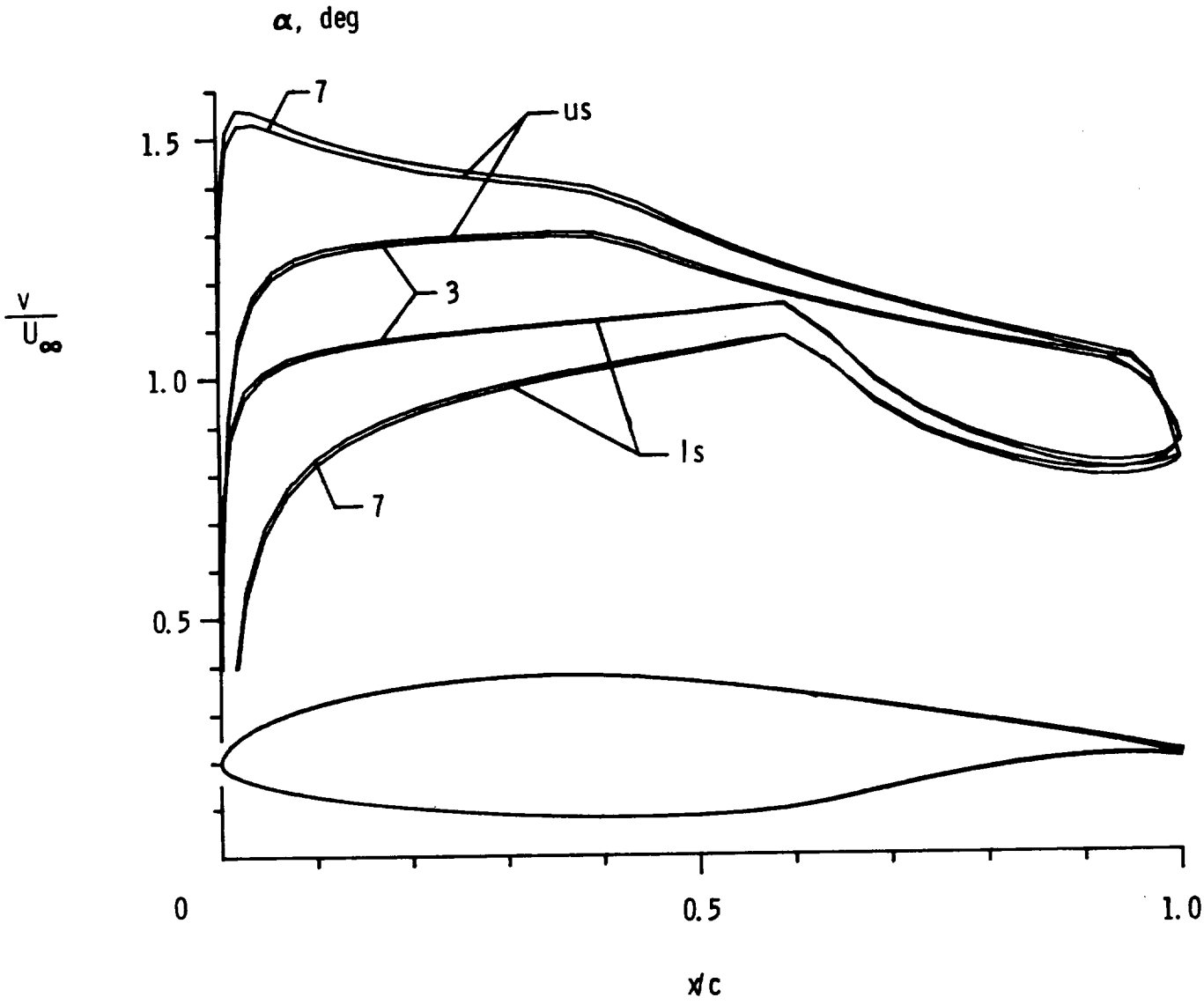

Figure 4. - Diagram with and without boundary-layer displacement iteration. (α relative to zero-lift line)